



The Goldfield Mining District, Nevada: An Acid-Sulfate Bonanza Gold Deposit

Barnaby W. Rockwell

United States Geological Survey
Denver, Colorado
<http://speclab.cr.usgs.gov>

October 2000

Forward

This paper provides an introduction to the geology, ore deposits, and fluid geochemistry of the Goldfield mining district, Esmeralda and Nye Counties, Nevada. Also included is a brief interpretation of mineral maps of the western half of the district which were recently produced from remotely sensed imagery acquired by the Airborne Visible Infrared Imaging Spectrometer (AVIRIS) system operated by NASA JPL.

Introduction and Mining History

The Goldfield mining district, located in the western Basin and Range province 250km north of Las Vegas, Nevada along U.S. Highway 95 (Figure 1), is one of most productive bonanza-grade epithermal mineral deposits hosted by hydrothermally altered Tertiary volcanic rocks in Nevada. Of this type of deposit, Goldfield ranks third in total gold, silver and copper production after the Comstock Lode and the Tonopah district, and second in gold production after Comstock (Ruetz, 1987). Float gold was discovered on Columbia Mountain in the western Goldfield Hills in 1902, and mining of the rich siliceous veins began in 1903. Production reached a peak in 1910, with 16.8 tonnes of gold and 3.67 tonnes of silver being shipped. After 1910, production steadily declined to below 0.62 tonnes of gold per year by 1920 (Ashley, 1974). By the time large-scale mining ceased in 1951, the Goldfield district produced 130 tonnes of gold, 45 tonnes of silver, and 16,870 tonnes of copper from about 4.2 million tonnes of ore, giving an average grade of 31 g/t Au (nearly 1 oz/t Au). Relatively small-scale mining operations in the 1980's focused on recovering lower-grade oxide ores (~ 2.2 g/t Au) from small open pits and old mine tailings (Ashley, 1990). It is estimated that at least 7 million tonnes of vein rock remain in the district with an average grade of about 3 g/t Au.

The Goldfield district lies within the central and western parts of the Goldfield Hills, a group of hills with elevations of 1,860 - 2,000 meters which is almost completely surrounded by lower desert basins at elevations of 1,450 - 1,600 meters. Maximum relief in the Goldfield Hills is about 300 meters (Ashley, 1974). The area is very sparsely vegetated by low grass, sage, and yucca.

The ore deposits at Goldfield are characteristic of the enargite-gold type (Berger, 1986), although at Goldfield the principal sulfosalt is famatinite (Cu_3SbS_4), the antimony-bearing analogue of enargite. These deposits, which can have significant byproduct copper, are

commonly hosted by calc-alkalic volcanic rocks which have undergone intense advanced argillic hydrothermal alteration in an epithermal environment (within several hundred meters of the surface at temperatures up to 300° C). Enargite-gold deposits are usually associated with subduction zones, island-arcs and back-arc spreading centers and often overlie porphyry copper deposits (Ashley, 1982; Sillitoe, 1983; Heald et al., 1987). Other examples of this type of

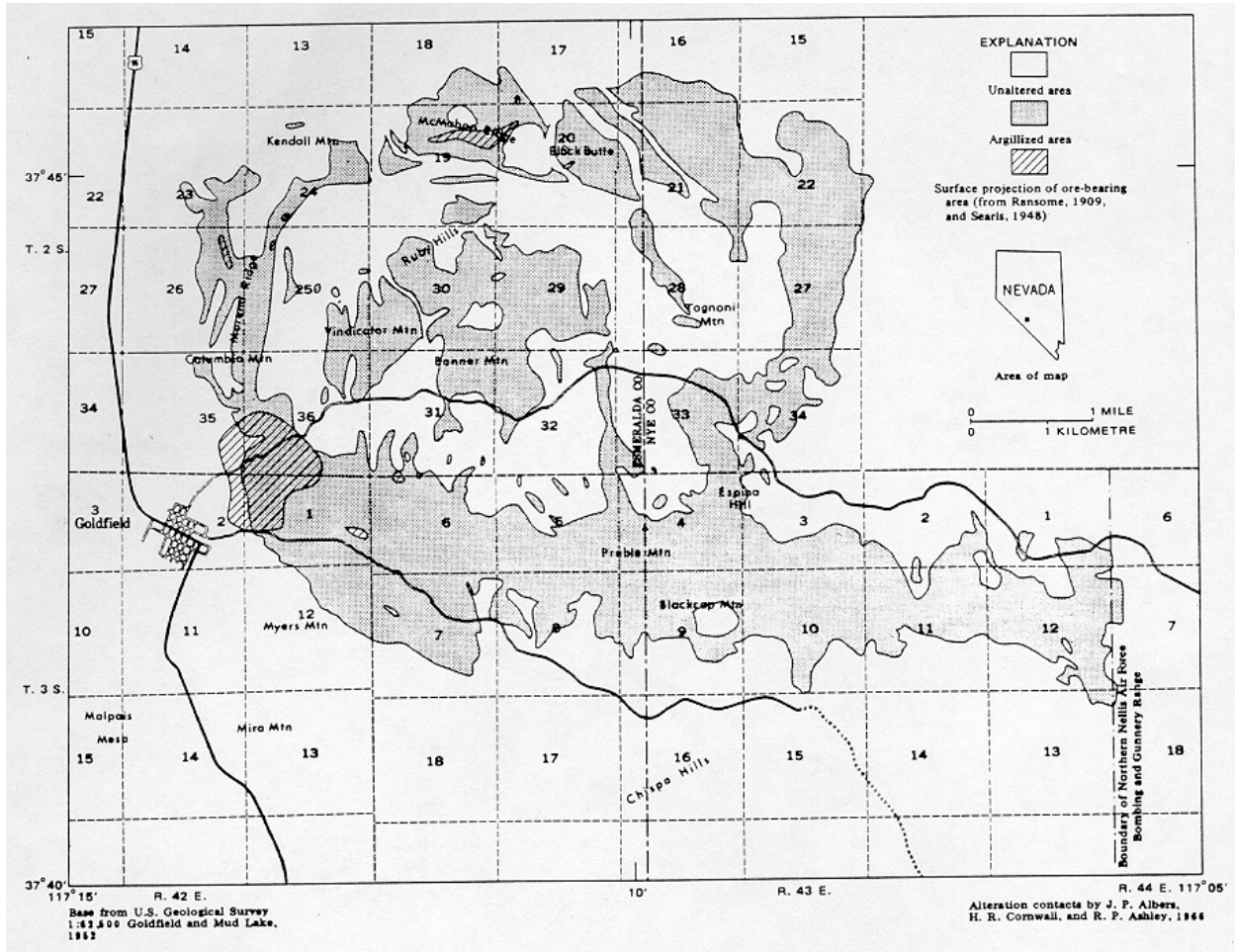


Figure 1. Map of Goldfield and vicinity showing areas of hydrothermal alteration and ore deposits (from Ashley and Keith, 1976).

Au/Ag/Cu deposit are: Red Mountain and Summitville, Colorado; Pyramid and Peavine-Wedekind districts, Nevada; El Indio, Chile; Julcani, Peru; Kasuga and Akeshi, Kyushu, Japan; and Chinkuashih, Taiwan. Although similar in host rock and ore/gangue mineralogy, the enargite-gold-massive sulfide deposits described by Sillitoe (1983) (Bor, Yugoslavia; Lepanto, Phillipines; Freida River, Papua New Guinea, etc.) are much larger than the Goldfield deposit.

Geologic Setting

The Goldfield Hills are a domed and intensely faulted uplift made up primarily of hydrothermally altered mid-Tertiary volcanic rocks of intermediate to felsic composition that host the mineralized vein systems (Figure 2). Unaltered late-Tertiary volcanic and sedimentary

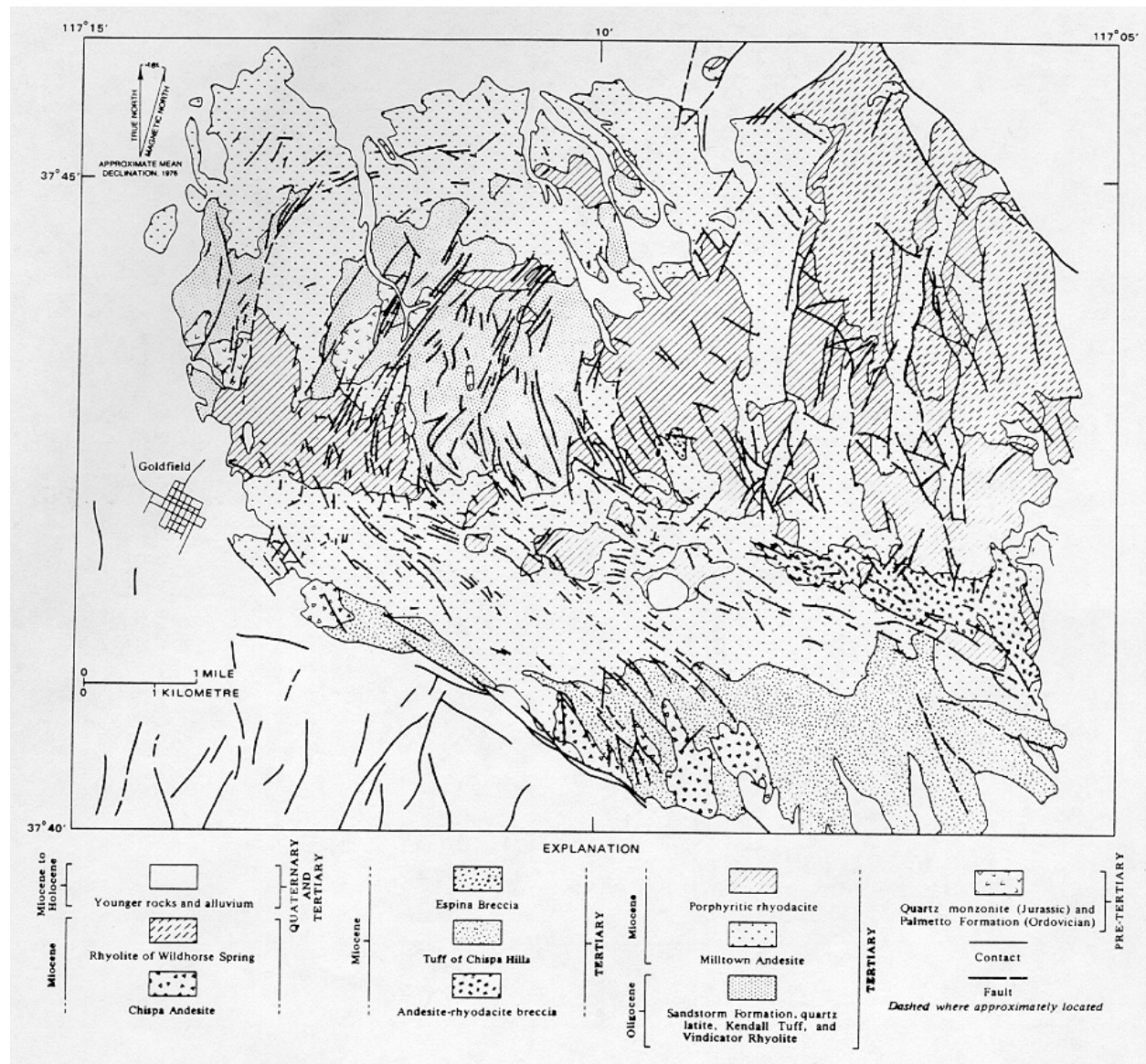


Figure 2. Generalized geologic map of the Goldfield mining district. From Ashley and Keith, 1976.

rocks fill the surrounding desert basins. The Goldfield district is considered the central vent complex from which many of the Tertiary volcanic rocks were extruded.

Stratigraphy - Black siliceous shales of the Ordovician Palmetto Formation (see Table 1), the oldest rocks in the area, have been intruded by Jurassic quartz monzonite and host minor amounts of ore in the deepest parts of the vein system (Ashley, 1990). These basement rocks are

Age	Formation/Event	Lithology/Occurrence	Exposure
Pliocene - Recent		Alluvium and pediment gravels	Surrounding basins and stream drainages
<i>EROSION</i>			
Middle Miocene - Lower Pliocene	Meda Rhyolite, Siebert Tuff, Thirsty Canyon Tuff, Malpais Basalt, etc.	Various tuffs, volcaniclastic sediments and basalts	Surround district
	Rhyolite of Wildhorse Spring	Non-altered	To east and northeast of elliptical fracture system
	Chispa Andesite	Non-altered trachyandesite flows and dikes	Myers Mountain and Chispa Hills to south
Lower Miocene (20-22 Ma)	ALTERATION & MINERALIZATION (~20.5 Ma)	Ore mainly in silicified zones	Ore mainly in western and northern parts of elliptical fracture system - argillic alteration around entire system
	Espina Breccia	Locally bedded rhyolite lapilli tuff and tuff breccia	Espina Hill
	Chispa Hills Tuff	Dacite vitrophyre of Ransome (1909) and rhyodacite ash-flow tuff	Chispa Hills south of elliptical fracture system
	Unnamed	Andesite-rhyodacite breccia	SE extension of elliptical fracture system
	Unnamed	ORE HOST. Porphyritic rhyodacite and rhyolite flow-dome complexes with minor tuff breccias	Tognoni, Preble and Columbia Mountains; Black Butte; to east of elliptical fracture system
	Milltown Andesite	Trachyandesite and rhyodacite flows, tuffs and breccias with minor quartz latite and basalt	Hydrothermally altered around circumference of elliptical fracture system
<i>UPLIFT and EROSION</i>			
Oligocene (30-31 Ma)	Sandstorm Rhyolite	Air-fall tuff and flow-dome	Banner Mountain and Ruby Hills
	Unnamed latite	Quartz latite flow-dome	
	Kendall Tuff	Quartz latite air-fall tuff	
	Morena Rhyolite	Ash-flow tuff	
	Vindicator Rhyolite	Silicic welded ash-flow tuff	
<i>UPLIFT and EROSION</i>			
Jurassic	Unnamed	Quartz monzonite	Vindicator & Columbia Mountains
Ordovician	Palmetto Fm.	Black siliceous shales, argillites and limestones	

Table 1. Stratigraphic column of the Goldfield mining district. Data from Ashley, 1974, 1979, and 1990; Ashley and Keith, 1976; and Ruetz, 1987.

exposed mainly in the central and western parts of the uplift on Vindicator and Columbia mountains (Figures 1 and 2).

The Tertiary volcanic rocks can be divided into three main groups based on age and composition (Ruetz, 1987). The first group consists of Oligocene calc-alkalic flows and tuffs dated at approximately 30-31 Ma which are exposed mainly on Banner Mountain and in the Ruby Hills in the central part of the district (Table 1). Silicic ash-flow tuffs of the Vindicator and Morena Rhyolites (Ransome, 1909) are the oldest rocks of this group and were deposited upon the eroded basement. It has been suggested that the extrusion of these units caused the subsidence of a caldera along a ring-shaped series of fractures about 6 km in diameter (Ashley, 1974 and 1990). These fractures acted as conduits for the migration of mineralizing fluids during the early Miocene. The elliptical shape of this system of fractures and related alteration is clearly visible in Figure 1 and Appendix A. Two additional tuffaceous units were extruded during the late Oligocene from vents along the elliptical fracture system, the first being of quartz latite composition (Kendall Tuff) from a vent 2 km east of Goldfield, and the second of rhyolitic composition (Sandstorm Rhyolite) from a vent on Morena Ridge north of Goldfield and another 2 km northwest of Tognoni Mountain. Each volcanic event was followed by the sealing of the vent(s) by a flow-dome. Later volcanism has obscured the true nature of the fracture system, however, and the existence of a caldera is a matter of interpretation (Romberger, 1992). No collapse breccias or other evidence for a local caldera are presented by Ashley (1979).

The second group of volcanic rocks unconformably overlies the first group and dates from the lower Miocene (20-22 Ma). These rocks are primarily intermediate in composition and have a total thickness of 600m. The Milltown Andesite is the oldest and most widespread unit of this group and its highly argillized trachyandesite and rhyodacite flows crop out around almost the entire elliptical fracture system. A unit of porphyritic rhyodacite and rhyolite (unnamed dacite of Ransome, 1909) intrudes and overlies the Milltown Andesite, forming flow-dome complexes in at least four centers around the elliptical fracture system (Ashley, 1979). This intrusive-extrusive unit is the host for most of the orebodies in the district. An unnamed sheet of coarse, andesite-rhyodacite breccia developed from the Milltown Andesite and porphyritic rhyodacite crops out at the eastern end of a linear east-trending extension of the elliptical fracture system. Several units of dacitic and rhyolitic tuff and tuff breccia overlie the lower Miocene volcanic rocks. Hydrothermal alteration and mineralization have been dated at c. 20.5 Ma and are closely related with this second group of volcanic rocks (Ruetz, 1987).

The third group of volcanic rocks dates from the mid-Miocene to lower Pliocene and post-dates most alteration and mineralization. These rocks are found around the periphery of the district outside of the elliptical fracture system and consist of various units of silicic tuffs, volcanoclastic sedimentary rocks and basalts. This bi-modal basalt-rhyolite suite is associated with Basin and Range faulting. This most recent group of volcanic rocks is overlain by Quaternary alluvium and pediment gravels.

Structure - At least five sets of faults are present in the Goldfield district. Although most of these faults were probably formed during early Miocene volcanism (Ashley and Keith, 1976), some may have been reactivated during Basin and Range deformation in the late Tertiary (Carrere, 1989). Many of the faults in the Goldfield district have served as conduits for fluid flow and are strongly silicified.

One set of faults is the most prominent and trends N30E across Vindicator Mountain, Banner Mountain and the Ruby Hills in the center of the district. These normal faults dip to the

east and have been interpreted as listric shingle faults bounding a series of rotated fault blocks; bedding and flow contacts within these blocks all dip to the west, away from the domed central part of the uplift (Ashley, 1990). A second set of faults trends nearly E-W (N80W) and defines the southern edge of the elliptical fracture system and its prominent 6 km-long eastward extension (Figures 1 and 2). These steeply dipping normal faults are also shingle faults, and bound south-dipping fault blocks. A third set of faults trends N20-40W and are readily visible where the ledges following these faults diverge from the highly altered, E-W-trending southern rim of the elliptical fracture system and march away towards the SE. The NE- and NW-trending sets of faults and fractures are most likely older structures, with the NW-trending set being related to the regional Walker Lane trend. A fourth set of faults is arcuate in form and appears to define the elliptical fracture system along its western and northwestern sides. These faults may represent re-activation of the late Oligocene ring-shaped fracture system, and may suggest a hinging effect in which the western half of the district was downdropped and rotated to a greater degree than the eastern half (S. Romberger, Colorado School of Mines, personal communication, 1998). As almost 95% of the ores were recovered from the western half of the Goldfield Hills, this hinging effect may have influenced the formation of the orebodies. In any case, the four sets of faults mentioned above intersect and interact in the vicinity of the main productive area, creating secondary permeabilities for enhanced fluid flow, alteration, and ore deposition. The fifth set of faults trend nearly N-S (N~10E) and appear to have been vital for focusing fluid flow in the central part of the district from Black Butte to Preble Mountain (see Figure 1).

It has been suggested that the faults in the Goldfield district are related parts of an interacting structural system (Byron Berger, USGS, personal communication, 2000). Differential movement along NW-trending, sub-parallel, right lateral shear zones to the north and south of the district are thought to have created a fault-bounded pull-apart basin of elliptical shape. The elliptical map pattern of alteration in the district may thus be due to fluid flow along the faults and fractures bounding this basin, rather than along faults related to the subsidence of a caldera.

Hydrothermal Alteration

Alteration in the Goldfield district is intense, widespread (greater than 40 km²), and well-exposed. For these reasons, the district has been well-mapped by airborne and satellite remote sensing systems (Carrere, 1989; Rockwell, 1997). The elliptical map pattern of the argillically altered Milltown Andesite is readily visible on Landsat Thematic Mapper (TM) satellite imagery processed for alteration detection (see Appendix A), and closely resembles the alteration pattern mapped by Ashley (1974) (Figure 1). Kaolinite, alunite, illite, chlorite, and montmorillonite, as well as various iron minerals, have been discriminated in the Goldfield district by airborne hyperspectral sensors such as the AVIRIS system designed and built by NASA's Jet Propulsion Laboratory.

Four distinct alteration assemblages have been recognized in the Goldfield district. These assemblages are summarized in Table 2. Pyrite enrichment can be found in all four assemblages. The assemblages occur in zoned envelopes around the resistant silicified ledges that formed along the faults, fractures or permeable beds which served as conduits for hydrothermal fluids: (1) an advanced argillic zone; (2) a phyllic-argillic zone; and (3) an argillic zone. The innermost advanced argillic zone serves as host for most, if not all, of the orebodies and is predominantly quartz, alunite, and OH⁻-bearing aluminosilicates. The advanced argillic zone can be subdivided

into two subzones based on quartz content: an inner, highly silicified and resistant zone which forms ledges along faults and fractures, and an outer, poorly-exposed zone containing less quartz which usually occurs on slopes beneath the ledges. The advanced argillic zones are strongly bleached in outcrop. Minerals present in the phyllic-argillic zone resemble a quartz-sericite-pyrite (QSP) assemblage except for the presence of abundant kaolinite. The argillic zone is enriched in quartz and clay minerals and grades from an inner, illite-rich zone to an outer zone enriched in montmorillonite.

Un- altered	Propylitic	Argillic		Phyllic- Argillic	Advanced Argillic		Highly Altered
	chlorite+ albite± epidote± mont.± calcite± zeolite± pyrite	<u>Mont- morillonite Subzone</u>	<u>Illite Subzone</u>	quartz+ kaolinite+ sericite± adularia± opal± pyrite	quartz±alunite ±kaolinite± pyrophyllite±sericite ±diaspore+leucoxene +pyrite		
		quartz+ mont.+ kaolinite+ illite± relict pyrite and feldspar	quartz+ illite+ kaolinite± adularia± opal± relict pyrite and feldspar		Poorly exposed - less quartz	Silicified ledges - high quartz content	

Table 2. Alteration assemblages in the Goldfield mining district. The argillic assemblages are strongly zoned around silicified veins and fractures, while the propylitic zone is patchy and discontinuous. Data from Ashley (1990) and Ruetz (1987).

Propylitic alteration is found farthest from the silicified ledges and is patchy and discontinuous in character (Ashley and Keith, 1976). The propylitization appears to be older than the hydrothermal alteration which produced the argillic assemblages. It may represent either an early phase of the primary alteration event, or an entirely different, older event possibly related to late Oligocene volcanism. The propylitic alteration is generally low in sulfides but varies significantly in mineral assemblage between host rocks, and may include diagenetic or deuteric alteration phases.

AVIRIS Data Reflectance Calibration

High altitude AVIRIS imagery was acquired over the Goldfield region on June 18, 1998. The AVIRIS data were calibrated to reflectance using a two step process (Clark et al., 1999). In the first step, the data are corrected using an algorithm (ATREM, Gao and Goetz, 1990 and Gao et al., 1992) that estimates the amount of atmospheric water vapor and other gases in the spectrum of each pixel independently, as compared with an atmospheric model. The algorithm uses this information to reduce the effects of absorptions caused by atmospheric water vapor on a pixel-by-pixel basis. This step also includes characterizing and removing the effects of Rayleigh and aerosol scattering in the atmosphere (path radiance), and a correction for the solar spectral response as a function of wavelength. The second step requires the in situ spectral

characterization of a ground calibration site which is present in the AVIRIS data coverage. The field site used for the calibration of the Goldfield AVIRIS data was the bright, montmorillonite-bearing soil of the Stonewall playa located 25 kilometers south of the town of Goldfield adjacent to the alteration center at Cuprite (Swayze, 1997). Additional areas of known composition were used to verify and further refine the accuracy of the calibration and to derive any residual path radiance correction.

Spectral Analysis of AVIRIS data

The USGS Tetracorder expert system was used for spectral analysis of the AVIRIS data (Clark et al., 1990, 1991, 1995). This software system compares the spectrum of each pixel in the AVIRIS data to a digital library of standard laboratory spectra of minerals, mineral mixtures, man-made materials, and vegetation. Each pixel is mapped separately for several different groups of surface materials, so that several maps can be generated for each AVIRIS dataset, including a map of iron-bearing minerals (0.35 to 1.35 micron spectral region), a map of phyllosilicate, sulfate, carbonate, and sorosilicate minerals (1.45 to 2.5 micron spectral region), and maps of man-made materials, snow, water, and vegetation. Mapping results are verified by both field checking and interactive comparison of AVIRIS spectra with library spectra.

Interpretation of Remotely Sensed Data

The AVIRIS-based mineral map of phyllosilicate, sulfate, carbonate, and sorosilicate minerals is shown in Appendix B. The ~17 meter ground resolution of the high altitude AVIRIS data is insufficient to resolve the silicified ledges which follow mineralized fracture zones. However, the distributions of medium- to coarse-grained hematite on maps of iron-bearing minerals produced from the AVIRIS data (not shown) can be used to indirectly infer the presence and abundance of the ledges. Around the district-wide elliptical zone of altered Milltown andesite, areas along ledge-topped ridges map as distinct patches of hematite within larger blankets of coarse-grained supergene jarosite derived from the weathering of pyrite from the ledges.

The main mining district (labelled "A" on the mineral map), located 1-2 kilometers NE of the town of Goldfield, is characterized by mixtures of kaolinite, illite/muscovite, and montmorillonite. The AVIRIS-based iron mineral mapping (not shown) indicates that fine-grained jarosite formed by the subaerial oxidation of pyrite is present in several of the mine waste rock piles in this area. Although coarse-grained, non-anthropogenic jarosite is common throughout the district, especially along the southern rim of the elliptical alteration pattern, a small occurrence of very pure jarosite located 1 kilometer east of Tognoni Mountain was mapped using AVIRIS data in the 2 micron spectral region (labelled "B" on the mineral map). Mapping jarosite in this spectral region with imaging spectroscopy data is difficult due to the overwhelming influence of OH absorption features in other minerals. The high degree of spectral purity of the jarosite in this area suggests that the rocks there have high contents of quartz and pyrite.

Most of the hills in the Goldfield region are underlain by resistant silicified and argillized rocks. Mixtures of kaolinite and illite/muscovite clearly outline the northern and part of the western sides of the district-wide elliptical alteration pattern. Mixtures of alunite and kaolinite

are dominant along Columbia Mountain and Morena Ridge in the west (see Figure 1), the Ruby Hills and Vindicator Mountain in the center, east of Tognoni Mountain, and along the entire southern rim of the alteration pattern. Most of the large occurrences of alunite are indicative of closely-spaced sets of mineralized fracture zones. These fracture zones coalesce into large "patches" of altered rock due to the scale of the AVIRIS pixels. The largest patches of alunite occur at the intersections of cross-cutting fracture zones. Preble Mountain (labelled "C" on the mineral map), a highly altered and silicified volcanic edifice located at the intersections of N80W and N20W-trending fracture systems, is underlain by potassium-rich alunite and mixtures of alunite and pyrophyllite, indicating that this area was an important high temperature center of the Miocene hydrothermal system. Sodium content of the alunite appears to increase away from Preble Mountain in all directions.

The clay mineral pyrophyllite occurs most often in areas where fractures are closely spaced and alteration is pervasive. Such areas also often occur at the intersections of cross-cutting sets of fractures. Exposures of pyrophyllite were mapped on the southern flanks of Vindicator Mountain, to the southeast and north of Banner Mountain, and in a small area along the southern rim of the alteration pattern (labelled "F" on the mineral map). Dickite occurs in silicified, resistant outcrops near the peripheries of certain advanced argillic alteration zones. Areas underlain by dickite appear to have very high concentrations of closely spaced fractures.

Between Banner and Tognoni Mountains (labelled "D" on the mineral map), large exposures of illite and chlorite were mapped with the AVIRIS data (the map showing chlorite and other iron minerals is not included here). A strong zonation with regard to aluminum content in the illites is evident, with low Al content illite occurring at the center of the zone, and increased Al content in the outer parts of the zone closer to the argillically altered rocks. Fractures are quite sparse in this area, suggesting that only weak argillic and/or propylitic alteration is prevalent. Patchy zones of chlorite attributed to propylitic alteration were remotely detected on the flanks of Vindicator and Columbia Mountains between argillically-altered and unaltered rocks (Rockwell, 1997). Propylitically altered rocks containing epidote, calcite, and muscovite were mapped just west and south of Black Butte along the northern rim of the elliptical alteration pattern (see "E" on mineral map).

Characteristics of the Ore Deposits

The bonanza orebodies occur as irregular sheets, pods, and pipes within the crudely tabular silicified zones which characterize the vein systems. The orebodies extend from the surface to a maximum depth of 410m (Ruetz, 1987). Approximately 95% of the ore was mined from a main productive area 1-2 km northeast of Goldfield (see Figure 1) from several east-dipping veins which decrease in dip angle and become more tabular with depth. These veins can be up to several meters in thickness (Buchanan, 1981). Subsidiary veins occur in both the hanging wall and footwall, and some of the hanging wall veins appear to splay upward from the main vein (Ashley, 1990). A zone of strong oxidation exists to depths of 30-40 m, but does not seem to have concentrated precious metals in a significant way (Ashley and Albers, 1975). The oxidation tends to obscure mineral zoning away from the main productive area.

The high grade ore occurred as open-space fillings in fractures and brecciated zones within highly silicified vuggy or "sooty" rock, and had grades up to 19,000 g/t Au (Ashley,

1974). Ore with grades over 3,110 g/ton Au were not uncommon in the district. These rich ores contained quartz, pyrite, famatinite (tetragonal $\text{Cu}_3(\text{Sb,As})\text{S}_4$) and other enargite/luzonite-group copper sulfosalts, goldfieldite ($\text{Cu}_6\text{Sb}_2(\text{S,Te})_9$), tetrahedrite-tennantite ($(\text{Cu,Fe,Ag})_{12}\text{Sb}_4\text{S}_{13}$), bismuthinite, gold-silver tellurides, and native gold. The richest orebodies were characterized by crustified breccia fragments coated with layers of these minerals, with gold occurring as one or more of the layers. The lower-grade ores (less than 31 g/t Au) consisted of fine-grained disseminated gold in silicified rock with subordinate pyrite and famatinite. High gold fineness is common in the Goldfield district, with an average gold/silver ratio of 3:1. Gold fineness decreases away from the main productive area. The ore mineralogy changes markedly with depth. With increasing depth, overall ore grades decrease, the degree of silicification decreases, concentrations of tellurides, bismuthinite, and famatinite decrease, and the abundances of silver, base metals and pyrite increase (Ruetz, 1987). The high-grade ores show anomalous concentrations of arsenic, antimony, bismuth, tellurium, lead, zinc, mercury, tin and molybdenum in addition to gold, silver, and copper (Ashley, 1990).

Mineral Paragenesis and Fluid Geochemistry

Ruetz (1987) has proposed a paragenetic sequence for the Goldfield district: pre-ore stage silica was deposited first, and was followed and overlapped by kaolinite and alunite, pyrite and marcasite, famatinite and tennantite, bismuthinite, goldfieldite and tellurides, and finally free gold overlapped by more silica. Vikre (1989) developed another paragenetic model for six alteration assemblages mapped at the Sandstorm and Kendall gold mines 3.2 km north of Goldfield. The six assemblages, ordered from oldest to youngest, are: (1) ledge replacement quartz, (2) barite and sulfides, (3) quartz + pyrite + barite, (4) quartz + barite + kaolinite breccia, (5) vuggy quartz, and (6) lateral replacement quartz. Gold was found to occur as inclusions in copper sulfosalts (including famatinite) and barite in assemblage (2), and in quartz and barite in assemblage (4). Vikre reported a wide range of homogenization temperatures ($100^\circ - 292^\circ \text{C}$), and salinities (0.2 - 7.9% weight percent NaCl equivalent). Studies of fluid isotopic compositions and salinities indicated that the mineralizing fluids contained pre-Miocene formational waters (probably modified seawater), meteoric waters, and magmatic waters (Vikre, 1989).

Secondary fluid inclusions in quartz phenocrysts from an advanced argillic alteration zone near Banner Mountain were used by Bruha and Noble (1983) for thermometric analysis. These studies found necked fluid inclusions with a wide range of homogenization temperatures, and suggested that the true temperature of formation was between $250^\circ - 290^\circ \text{C}$. Five different daughter minerals were present, and the average salinity of the fluids was 7 weight percent NaCl equivalent. Dissolved salts included NaCl, KCl, CaCl_2 , MgCl_2 and FeCl_2 . Widely variable salinities were attributed to mixing with meteoric waters in a shallow environment, but the high chloride contents indicated that the hydrothermal acid-sulfate solutions were derived from depth. Ashley (1979) cited $\delta^{18}\text{O}$ values of -12% as evidence for the involvement of meteoric waters, and interpreted $\delta^{34}\text{S}$ values near 0% as evidence for a magmatic sulfur source derived from the deep crust or upper mantle. The very large amount of gold and sulfur in the deposit also suggests that they were derived from a deep source. Taylor (1973) found abundant evidence of boiling.

Sulfur isotopic evidence for both hypogene and supergene alunite has been found. Hypogene replacement alunites exhibited $\delta^{34}\text{S}$ values between +11.6 and +23.3 per mil, indicating sulfide/sulfate fractionation at temperatures of 150 °C or higher (Jensen et al., 1971). Some vein alunites had $\delta^{34}\text{S}$ values near 0.0 per mil, indicating that they were formed by the oxidation of pyrite during supergene alteration (Ashley, 1990).

Genetic Model

Buchanan (1981) proposed that the episodic boiling of convecting fluids in a shallow, low-temperature, hot springs environment could explain many of the observed features of "epithermal" ore deposits. In his model, deeply circulating meteoric waters mix with magmatic fluids and dissolve metals, alkalis, chlorides, and sulfur species from the volcanic/sedimentary pile. These low-salinity fluids then rise through fracture systems and deposit ore and gangue material as fracture fillings and replacements in wall rocks. A magma body at several kilometers depth provides the heat engine which drives the hydrothermal system (Figure 3).

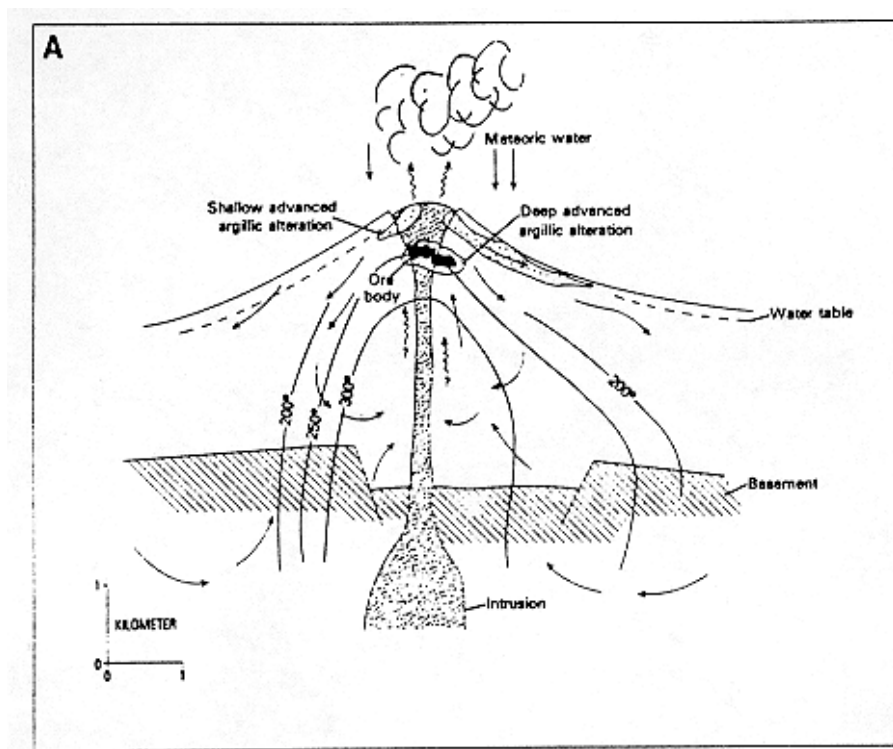


Figure 3. Occurrence model of an acid-sulfate type epithermal ore deposit. The wiggly arrows represent sulfur-rich emanations from the intrusion. From Heald et al, 1987.

There are three distinct stages involved in the genesis of the ore deposits at Goldfield. Systems of pervasive, interacting faults and fractures must exist for providing the secondary permeabilities required for enhanced fluid flow. The first stage involves the development of pre-ore stage acid-sulfate alteration by magmatic steam-related processes. This alteration prepares the ground in two ways: 1) greatly reducing the buffering capacity of the rocks, which allows for the stability of the highly acidic fluids required for ore-grade metal solubilities and transport, and

2) the leaching of many minerals by acidic fluids leaves silica-rich rocks which are more competent and prone to the development of secondary permeability by brittle fracture. The second stage involves the development of a convecting hydrothermal system and the deposition of rich siliceous ores in open conduits. The third stage involves the continued deposition of metals by circulating steam-heated water.

In magmatic hydrothermal acid sulfate alteration systems, a magma body releases gaseous plumes rich in SO₂ which rise through faults and fractures and eventually mix with meteoric waters to form a hydrothermal system characterized by high sulfur activities (Ashley, 1990; Rye et al., 1992). In these systems, rising magmatic SO₂ mixes with meteoric water and disproportionates to H₂S vapor and sulfate, eventually leading to the production of H₂SO₄ (Heald et al., 1987). More oxidizing environments can also promote the formation of sulfate. The sulfuric acid is responsible for the intense hypogene hydrolytic alteration and leaching which characterize most enargite-gold deposits. The hydrothermal systems can become locally clogged with precipitated silica near the paleosurface. A build-up of hydraulic pressure or seismic activity can cause failure of the cap rock (or sinter) through fracturing and brecciation, leading to catastrophic decompression and flash boiling of the fluids. Such episodic flash boiling could be responsible for the layered and crustiform textures of the high-grade bonanza ores.

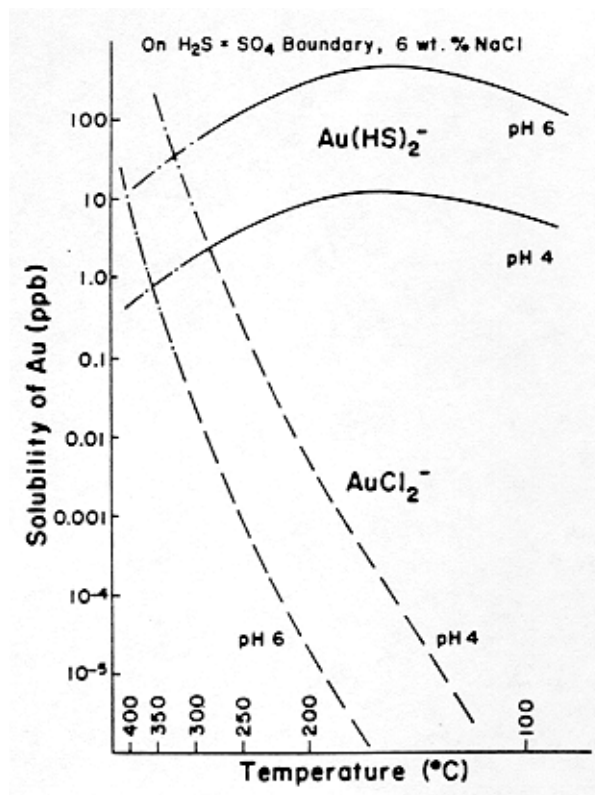


Figure 4. Aqueous solubility of gold as a function of temperature and pH along the H₂S-sulfate boundary in a 6 weight % NaCl solution. Bisulfide complexes are shown as solid lines and chloride complexes are shown as dashed lines. From Romberger, 1990.

Boiling is a key process for the formation of bonanza gold deposits. Ewers and Keays (1977) found that the zoning of metals in a modern hot springs hydrothermal system is a function of the boiling level in that system. Base metals, silver and gold are very soluble as chloride complexes above 300 °C, but base metals are relatively insoluble below 300 °C (Large et al., 1989; Romberger, 1990) (see Figure 4). Therefore, base metals and silver will precipitate at relatively higher temperatures at and below the boiling level. Gold is soluble from 90 °C to 175 °C as bisulfide complexes and will thus precipitate at or above the boiling level. Mixed metal zones can thus be formed at the boiling level. This process may account for the vertical segregation of metals within the veins at Goldfield.

The stippled area in Figure 5 indicates that the solutions straddle the boundary between the stability fields of pyrite and hematite. Pyrite is found throughout the alteration zones at Goldfield (Table 2). The pyrite can be formed by two reactions: 1) a relatively small amount of pyrite is formed during the breakdown of the gold-bisulfide complexes caused by reactions with

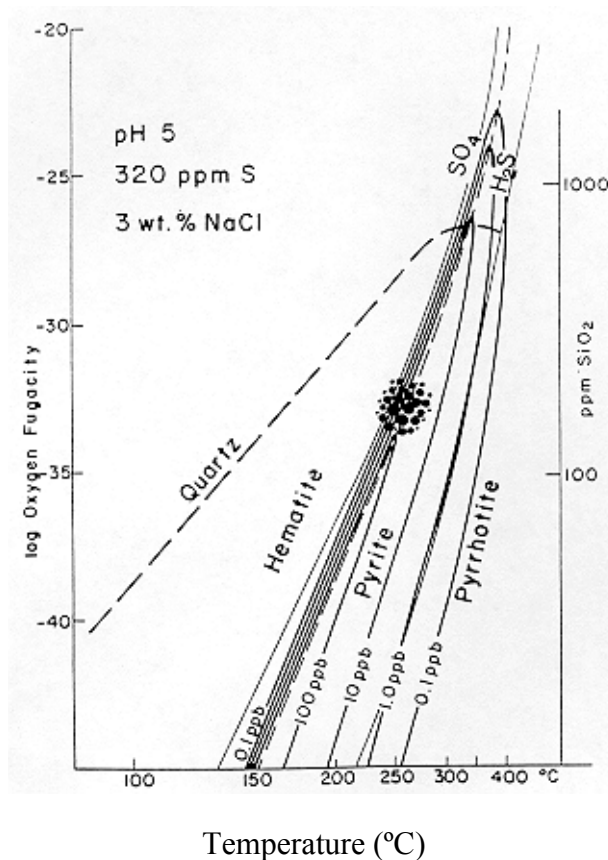


Figure 5. Aqueous solubility of gold and silica as a function of temperature and oxygen activity at pH 5 in solutions containing 320 ppm sulfur (0.01 molal) and 3 wt. % NaCl (0.5 molal). Heavy solid lines are for gold bisulfide complexes. The boundary between the aqueous sulfate and sulfide field is shown as a fine dashed line. The stippled area represents the physicochemical composition of a suggested average fluid responsible for mineralization in bonanza gold deposits. From Romberger, 1992.

iron oxides from the host rocks or with dissolved ferrous iron; and 2) the combination of ferrous iron from the host rocks with dissolved sulfur from the H₂S (Romberger, 1990). In an epithermal system such as Goldfield, pyrite can be introduced during each of the three stages of mineralization mentioned above (Byron Berger, USGS, personal communication, 2000). Near-surface oxidation of pyrite creates additional sulfuric acid and the often intense limonitic staining (goethite and jarosite) found within the argillically altered and silicified rocks at Goldfield. This sulfuric acid will percolate downwards, leaching the K- and Al-rich volcanic rocks to produce supergene alunite and jarosite with $\delta^{34}\text{S}$ values near 0.0 per mil. The stability field of hematite is reached when the rising fluids cool to about 240° C and become more oxidized with sulfate being the stable sulfur species (Figure 5). Hypogene hematite will be deposited from the mineralizing solution upon further cooling and oxidation, but may be removed during acid supergene alteration. Intergrown crystals of alunite and jarosite found on Preble Mountain were interpreted as evidence for hypogene jarosite by Keith and Ashley (1979), although it is highly likely that most of the jarosite present on the surface in alunitic zones at Goldfield has a supergene origin due to the abundance of pyrite in the advanced argillic zones of “high sulfidation” magmatic hydrothermal systems.

The zoned alteration assemblages observed adjacent to silicified ledges at Goldfield represent progressive reactions between the hot fluids in a fracture system and the wall rocks. The fluids are acidic and have high temperatures and sulfur activities, and the wall rocks near the fractures are entirely leached and replaced with alunite. Where pervasive fracture systems focus fluid flow, pyrophyllite may form within the alunitized rocks. Farther from the fractures, increased wall rock buffering of the fluids increases pH while the fluid temperature decreases, leading to the formation of the zoned suite of clay minerals (Table 2). At the edges of the hydrothermal system, where fracture control, rather than replacement, becomes the primary physical factor of mineralization, dickite can form along with introduced silica. The abundant fractures in these areas focus fluid flow and provide the high temperatures (150° - 270° C) required for the formation of dickite rather than kaolinite. Over time, metals are deposited in the zones of highest permeability along with silica leached from rocks lower in the system.

The presence of faults and fractures in the hanging walls of the vein systems is important for allowing the hydrothermal system to recharge with meteoric water. These hanging wall faults are often mineralized, and help to produce more developed alteration halos in the hanging walls than are typically found in the footwall rocks. However, where the ledges are sub-parallel and closely spaced, the footwall of one fault is the hanging wall of another, and the above relationship is obscured.

Conclusions

A suite of geologic features and physicochemical conditions are essential for the formation of bonanza-grade enargite-gold deposits characterized by intense acid-sulfate alteration. First, a calc-alkalic magma must intrude to shallow depths to provide both the heat required to drive the hydrothermal system and the sulfur required for the formation of the acidic fluids necessary for alteration and ore deposition. Second, a set of permeable zones must exist in which formational, magmatic and meteoric waters will be focused and be able to mix and flow. These permeable zones can consist of faults, fractures, or permeable beds. Third, these permeable zones must remain open and under hydrostatic pressure for significant lengths of time

to allow for the formation of the banded and crustiform textures often found in the high-grade orebodies.

Enargite-gold deposits are commonly associated with domes or flow-domes of porphyritic, felsic to intermediate volcanic rocks of mid- to late-Tertiary age (Ashley, 1982). The calc-alkalic rocks are susceptible to brittle fracturing at shallow depths and will thus act as prime host rocks for mineralization. In addition, these silica-rich magmas can provide abundant silica to the mineralizing fluids. Early alteration of host rocks serves as ground preparation for bonanza mineralization: the leached, silica-rich rocks are more competent and prone to brittle fracture, and the residual acid-sulfate alteration assemblages have greatly reduced capacities for fluid pH buffering. Island arcs and back-arc spreading centers associated with subduction zones at continental margins will provide both the calc-alkaline volcanic rocks and the structural stress regimes favorable for the development of these deposits. Fracture permeability will be maintained by both tectonic breakage and by episodic hydraulic fracturing (Ashley, 1990).

Remote sensing technologies are a valuable tool for mapping the extent and types of alteration in exposed ancient and modern hydrothermal systems. Landsat imagery is a cost effective tool for reconnaissance alteration mapping on a regional scale, and hyperspectral imaging can be used to generate detailed, large-scale maps of alteration assemblages which can be used, in conjunction with structural mapping, to define local target areas most favorable for further geochemical sampling and drilling programs.

References

- Ashley, R.P., 1974, Goldfield mining district, in Guidebook to the geology of four Tertiary volcanic centers in central Nevada: Nevada Bureau of Mines and Geology Report 19, p. 49-66.
- Ashley, R.P., 1979, Relation between volcanism and ore deposition at Goldfield, Nevada, *in* Papers on Mineral Deposits of Western North America: Nevada Bureau of Mines and Geology Report 33, p. 77-86.
- Ashley, R.P., 1982, Occurrence model for enargite-gold deposits, *in* Erickson, R.L., compiler, Characteristics of mineral deposit occurrences: U.S. Geological Survey Open-File Report 82-795, p. 144-147.
- Ashley, R.P., 1990, The Goldfield gold district, Esmeralda and Nye counties, Nevada, *in* Epithermal Gold Deposits - Part I: U.S. Geological Survey Bulletin 1857-H, pp. H1-H7.
- Ashley, R.P. and Albers, J.P., 1975, Distribution of gold and other ore-related elements near ore bodies in the oxidized zone at Goldfield, Nevada: U.S. Geological Survey Professional Paper 843-A, 48 p.
- Ashley, R.P. and Keith, W.J., 1976, Distribution of gold and other metals in silicified rocks of the Goldfield mining district, Nevada. Geological Survey Professional Paper 843-B, 17 p.

- Berger, B.R., 1986, Descriptive model of epithermal quartz-alunite Au, *in* Cox, D.P., and Singer, D.A., eds., Mineral Deposit Models: U.S. Geological Survey Bulletin 1693, p. 158.
- Bruha, D.J. and Noble, D.C., 1983, Hypogene quartz-alunite±pyrite alteration formed by moderately saline, ascendant hydrothermal solutions: Geological Society of America Abstracts with Programs, v. 15, no. 4, p. 325.
- Buchanan, L.J., 1981, Precious metal deposits associated with volcanic environments in the southwest, *in* Dickinson, W.R. and Payne, W.D., eds., Relations of Tectonics to Ore Deposits: Arizona Geological Society Digest, v. 14, pp. 237-262.
- Carrere, V., 1989, Mapping alteration in the Goldfield mining district, Nevada, with the Airborne Visible/Infrared Imaging Spectrometer (AVIRIS), *in* Proceedings, International Symposium on Remote Sensing of Environment, Seventh Thematic Conference: Remote Sensing for Exploration Geology, Calgary, Alberta, Canada, October 2-6: ERIM, Ann Arbor, MI.
- Clark, R.N., A.J. Gallagher, and G.A. Swayze, 1990, Material absorption band depth mapping of imaging Spectrometer data using a complete band shape least-squares fit with library reference spectra: *in* roceedings of the d Airborne Visible/Infrared Imaging Spectrometer (AVIRIS) Workshop, JPL Publication 90-54, pp. 6-186.
- Clark, R.N., G.A. Swayze, A. Gallagher, N. Gorelick, and F. Kruse, 1991, Mapping with imaging spectrometer data using the complete band shape least-squares algorithm simultaneously fit to multiple spectral features from multiple materials: *in* Proceedings of the Third Airborne Visible/Infrared Imaging Spectrometer (AVIRIS) Workshop, JPL Publication 91-28, pp. 2-3.
- Clark, R.N. and G.A. Swayze, 1995, Mapping minerals, amorphous materials, environmental materials, vegetation, water, ice and snow, and other materials: The USGS Tricorder Algorithm: *in* Summaries of the Fifth Annual JPL Airborne Earth Science Workshop, January 23- 26, Pasadena, CA, R.O. Green, Ed., JPL Publication 95-1, pp. 39-40.
- Clark, R.N., G.A. Swayze, T.V.V. King, K.E. Livo, R.F. Kokaly, J.B. Dalton, J.S. Vance, B.W. Rockwell, and R.R. McDougal, 1999, Surface reflectance calibration of terrestrial imaging spectroscopy data: a tutorial using AVIRIS, USGS Open File Report 99-xx. In press. Available online at:
<http://speclab.cr.usgs.gov/PAPERS.calibration.tutorial/calibntA.html>
- Ewers, G.R. and Keays, R.R., 1977, Volatile and precious metal zoning in the Broadlands geothermal field, New Zealand: ECON. GEOL., v. 72, no. 7, pp. 1337-1354.
- Gao, B.C. and A.F.H. Goetz, 1990, Column atmospheric water vapor and vegetation liquid water retrievals from airborne imaging spectrometer data: J. Geophys Res. 95, pp. 3549-3564.

- Gao, B.C., K.B. Heidebrecht, and A.F.H. Goetz, 1992, ATmospheric REMoval Program (ATREM) User's Guide, version 1.1, Center for the Study of Earth From Space document, University of Colorado, 24pp.
- Heald, P., Foley, N.K., and Hayba, D.O., 1987, Comparative anatomy of volcanic-hosted epithermal deposits: acid-sulfate and adularia-sericite types: *ECON. GEOL.*, v. 82, no. 1, pp. 1-26.
- Jensen, M.L., Ashley, R.P., and Albers, J.P., 1971, Primary and secondary sulfides at Goldfield, Nevada: *ECON. GEOL.*, v. 66, pp. 618-626.
- Keith, W.J., Calk, L., and Ashley, R.P., 1979, Crystals of coexisting alunite and jarosite, Goldfield, Nevada: U.S. Geological Survey Professional Paper 1124-C.
- Large, R.R., Huston, D.L., McGoldrick, P.J., and Ruxton, P.A., 1989, Gold distribution and genesis in Australian volcanogenic massive sulfide deposits and their significance for gold transport models: *ECON. GEOL. Monograph* 6, pp. 520-536.
- Ransome, F.L., 1909, Geology and ore deposits of Goldfield, Nevada: U.S. Geological Society Professional Paper 66, 258 p.
- Rockwell, B.W., 1997, Hydrothermal Alteration Mapping using Landsat Thematic Mapper and GER 63-Channel Imaging Spectrometer Data, *in* Mining Opportunity Bulletin, Remote Sensing Supplement, Randol International, Golden, CO, quarter 2, vol. 4, no. 2.
- Romberger, S.B., 1988, Geochemistry of gold in hydrothermal deposits: U.S. Geological Survey Bulletin 1957-A, p. A9-A25.
- Romberger, S.B., 1990, Geochemistry of epithermal precious metal deposits, *in* Hausen, D.M., ed., Gold '90: Society of Mining, Metallurgy, and Exploration, Inc., Littleton, CO, pp. 181-187.
- Romberger, S.B., 1992, A model for bonanza gold deposits, *in* Sheahan, P.A., and Cherry, M.E., eds., Ore Deposit Models, Volume II: Geological Association of Canada Reprint Series 6, pp. 77-86.
- Ruetz, J.W., 1987, The geology of the Goldfield district, *in* Johnson, J.L., ed., Bulk mineable precious metal deposits of the western United States: Geological Society of Nevada, Guidebook for Field Trips, pp. 114-119.
- Rye, R.O., Bethke, P.M., and Wasserman, M.D., 1992, The stable isotope geochemistry of acid sulfate alteration: *ECON. GEOL.*, v. 87, no. 2, pp. 225-261.
- Searls, F., Jr., 1948, A contribution to the published information on the geology and ore deposits of Goldfield, Nevada: Nevada University Bulletin, v. 42, no. 5 (Geology and Mining Series 48), 24 p.

- Sillitoe, R.H., 1983, Enargite-bearing massive sulfide deposits high in porphyry copper systems: ECON. GEOL., v. 78, pp. 348-352.
- Swayze, G.A., 1997, "The hydrothermal and structural history of the Cuprite Mining District, Southwestern Nevada: An integrated geological and geophysical approach," Ph. D. Dissertation, University of Colorado, Boulder, Colorado, p. 399.
- Taylor, H.P., Jr., 1973, O¹⁸/O¹⁶ evidence for meteoric-hydrothermal alteration and ore deposition in the Tonopah, Comstock Lode, and Goldfield mining districts, Nevada: ECON. GEOL., v. 68, pp. 747-764.
- Vikre, P.G., 1989, Ledge formation at the Sandstorm and Kendall gold mines, Goldfield, Nevada: ECON. GEOL., v. 84, pp. 2115-2138.

Appendix A

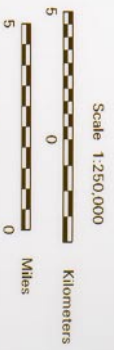
Reconnaissance Mineral Exploration using Landsat Thematic Mapper (TM) imagery:
Goldfield Region, Nevada, USA



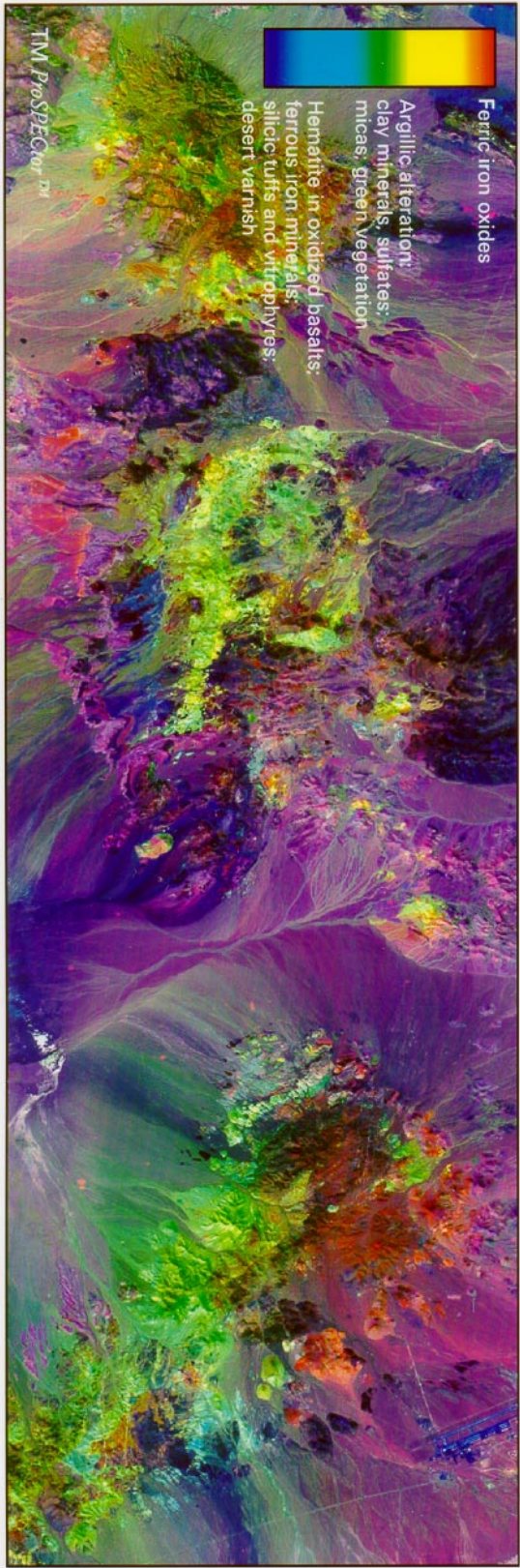
Barnaby W. Rockwell

Reconnaissance Mineral Exploration
using Landsat Thematic Mapper (TM) Imagery:
Goldfield Region, Nevada, USA

Landsat WRS 41/33, acquired July 4, 1991. Image precision geocoded to Transverse Mercator projection, UTM Zone 11, Clark 1866 ellipsoid



TM 321/RGB True-Color Composite

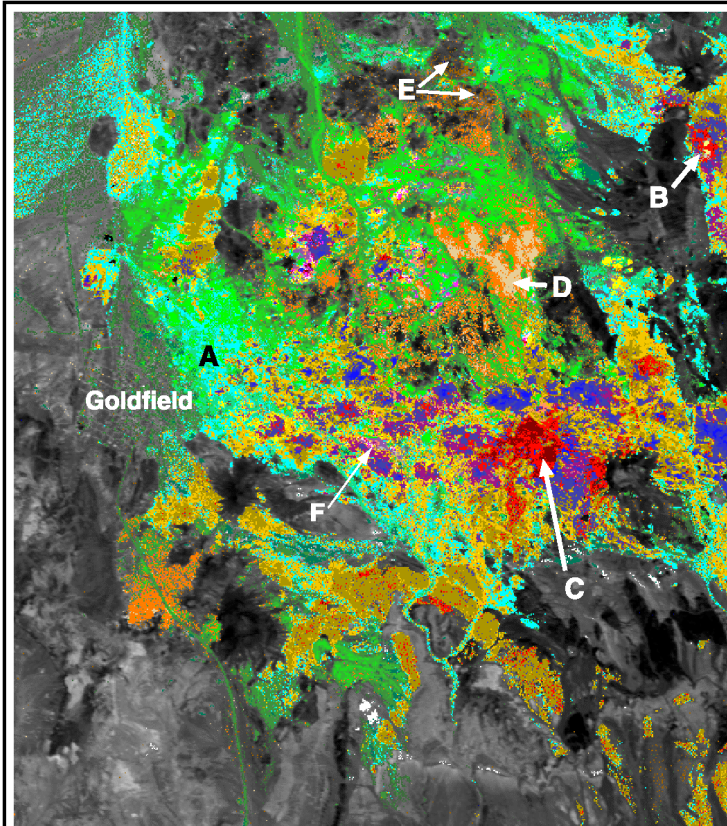


- Ferric iron oxides
- Argillic alteration: clay minerals, sulfates; micas, green. Vegetation
- Hematite in oxidized basalts; ferrous iron minerals; siliceous tuffs and vitrophyes; desert varnish

TM ProSPECTOR TM

Appendix B

High altitude AVIRIS mineral map:
Phyllosilicate, Sorosilicate, Carbonate, and Sulfate Minerals



NEWCOLOR

Goldfield, Nevada

AVIRIS 1998 Data
gf98_r2s5-6.rtg

Tetracorder 3.6a6 Product

Barnaby W. Rockwell

Phyllosilicates, Sulfates, Sorosilicates, and Carbonates

